Materials Science Forum
ISSN: 1662-9760, Vol. 848, pp 505-518
doi:10.4028/www.scientific.net/MSF.848.505

Synthesis of Silicon Microspheres

Lianyun Liu[1, a], Tingting Zhang[1, b], Hui Zhang[1, c*], Xiaxia Bai[1, d] and Stefano Polizzi[2, e]

[1]School of Science, Beijing Jiaotong University, Beijing 100044, China

[2]Dipartimento di Scienze Molecolari e Nanosistemi, Universita' Ca' Foscari Venezia, Venezia-Mestre 30123, Italy

[a]lyliu@bjtu.edu.cn, [b]14126067@bjtu.edu.cn, [c]hzhang1@bjtu.edu.cn, [d]14126058@bjtu.edu.cn, [e]polizzi@unive.it

Keywords: Silicon, Microspheres, Synthesis.

Abstract. The synthesis of silicon microspheres is of outmost importance, especially for the production of optical and electrical devices due to their unique properties displayed by this material. In this paper, we review the research on the synthesis of silicon microspheres, including one physical method, the drop method and several chemical methods, such as vapor-phase reaction, vapor-solid reaction, liquid phase reaction and magnesio-thermal reduction method. The formation mechanisms for silicon microsphere particles are also summarized.

Introduction

As is well known, silicon is a raw material in many industrial sectors as metallurgy, electronics, and photonics. It has been widely used in the microelectronic industry [1, 2] for producing semiconductor devices for more than half a century. Silicon is transparent to near-IR light due to its bandgap of 1.1 eV and its high refractive index (n = 3.48) increases the optical path-width and makes it possible to use it for the production of smaller devices [3]. Therefore, silicon can be also used for the production of special optical devices as photonic crystals [4-6], waveguides [7-9], multiplexers [10], and nano-lasers [11, 12]. Recently, the photovoltaic industry has seen a rapid development due to increasing efforts in environment preservation. In particular, spherical silicon solar cells, based on small-size crystalline silicon microspheres have attracted considerable interest for saving the silicon feedstock and realizing low-cost photovoltaic modules [13-16]. Silicon microspheres can also be used for detectors, modulators, and optical switching because silicon-based Raman lasers can overcome those shortcomings such as large nonlinear optical losses and low output efficiency existing in conventional Raman lasers [17-20]. In addition, silicon microspheres have received much attention within the optical micro cavity resonator community because microspheres possess high quality factor (Q-factor) morphology-dependent resonances (MDR), i.e. whispering gallery modes (WGMs) [11], which make them suitable for applications in this field. It is worth mentioning that spherical silicon composites show promising applications as anodes for next-generation Li-ion batteries, due to their lower irreversible capacity, higher energy density, and good process-ability [21, 22].

The synthesis of silicon microspheres with controlled morphology is of outmost importance. Researchers have carried out investigations on the preparation of silicon microspheres by various processes, and many efforts have been made to obtain silicon microspheres of relatively uniform sizes and smooth surfaces. It is crucial to investigate the growth process in order to achieve higher material quality and a number of studies have been dedicated to the mechanisms of preparation of silicon microspheres. This paper provides a review of the synthesis procedures for obtaining silicon microspheres, covering both physical and chemical methods. The paper also provides a brief review of the formation mechanisms of silicon microspheres produced by decomposition of silicon hydride.

Synthesis of Silicon Microspheres

Synthesis processes of silicon microspheres may involve physical methods, such as the drop method, or chemical methods, such as vapor-phase reaction method, liquid-phase reaction method, and others. Table 1 gives the comparison of different synthesis methods. This section provides a detailed introduction to the most common ones of them.

Table 1 Comparison of different synthesis methods

Methods	The morphologies and sizes of silicon microspheres	References
Drop method	Diameter: 1 mm, rough or smooth surfaces	[23]
Vapor phase reaction method	Diameter: 20~40 nm, narrow size distribution	[24]
Vapor-solid phase reaction method	Diameter: 0.5~5 μm, smooth surface	[25]
Liquid phase reaction method	Diameter: 200~300 nm, non-agglomerated spheres	[26]
Magnesiothermal reduction method	Diameter: 300~400 nm, porous spheres	[27]

Physical Methods

The drop method. The most commonly used physical method to produce silicon microsphere particles is the drop method [28, 29]. The main advantage of this method is that crystals can be fabricated directly from molten silicon without chemical reactions and the risk of explosive hazards. However, a complex experimental apparatus and high temperatures are needed; furthermore, the spherical silicon fabricated by this method has usually a rather poor crystallinity and it is not uniform in quality.

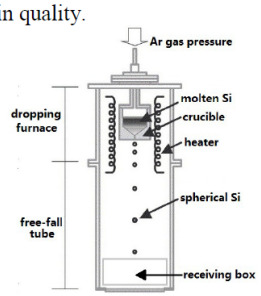

Fig. 1 Schematic diagram of the experimental apparatus used for the drop method [30].

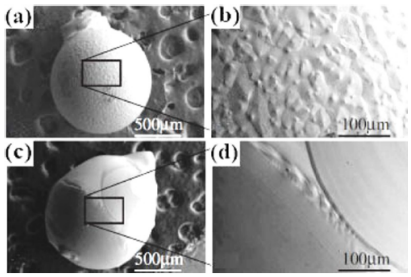

Fig. 2 Surface morphology of silicon microspheres with (a) (b) rough and (c) (d) smooth surfaces fabricated by the drop method [23].

Fig. 1 shows a schematic diagram of the experimental apparatus [30]. It consists of a dropping furnace and a free-fall tube, including a crucible with a nozzle at the bottom, a receiving box and heaters. First, the source material is filled in the crucible and is melted with heaters. Then, the silicon melt is driven towards the nozzle by the pressure of an inert gas to form droplets. The inert gas atmosphere in the dropping area is important, because it is effective for decreasing impurities concentration. The droplets are cooled down by ambient Ar gas in the free-fall tube and they solidify into spherical silicon particles by surface tension. In order to obtain high quality silicon microspheres, it is crucial that molten silicon droplets solidify at low undercooling conditions and with a low cooling rate. The silicon microspheres are finally accepted by a receiving box mounted at the end of the free-fall tube. Fig. 2 shows the surface morphology of silicon microspheres of 1mm in diameter with (a) (b) rough and (c) (d) smooth surfaces fabricated by the drop method [23]. Because the silicon microspheres formed by this method generally had poor crystallinity, containing high-density grain boundaries, point defects, and dislocations [31-33], some researchers have been working on improving their quality and the yield [29, 34-37]. For instances, Liu *et al.* [34] developed a novel seeding crystallization technique by ejecting silicon powders onto the molten silicon droplets and they obtained silicon microspheres with a size distribution around 1.0 mm in diameter. Kuzuokaa *et al.* [35] studied the relationship between the fabricating conditions and the

resulting. By controlling the cooling rate, high quality spherical silicon particles, which consisted of 2-3 grains, were obtained. Huang *et al.* [29] reported a new approach, namely, a melting and recrystallization process of the particles formed by the drop method. The silicon droplets were recrystallized under different super-cooling conditions and spherical silicon single crystals, free of defects, were grown successfully in the super-cooling range of 285K-315 K.

Chemical Methods

Silicon precursors and diluents. Silicon microspheres can be also prepared through chemical methods. Silicon precursors and diluents are needed for certain chemical methods, such as vapor phase reaction method and vapor-solid phase reaction method. In the early days, several gases were explored as precursors for the synthesis of silicon microspheres, but monosilane SiH_4 and trichlorosilane $SiHCl_3$ are the ones most frequently used now. The main reasons for using monosilane are the relatively low pyrolysis temperature and the absence of reverse reactions. The thermal decomposition temperatures of SiH_4 and $SiHCl_3$ are about 693K and 741K, respectively [38]. However, decomposition reaction often operates at higher temperatures than the decomposition one to assure the formation of a crystalline structure [39]. Moreover some intermediate silicon chlorides need higher temperatures to decompose and low-temperature amorphous structures might reduce the quality of the material [40]

Three main diluents are generally used in preparing silicon microspheres: hydrogen, argon and helium. Diluents are primarily employed to reduce the number concentration of particles and to slow down decomposition rate so as to prevent particles from growing large and avoiding agglomeration [41, 42]. In addition, diluents may have a considerable effect on gas-phase reactions. For example, an inert ambient largely promotes homogeneous reactions of SiH_4, whereas a hydrogen atmosphere decreases the homogeneous nucleation rate [42, 43]. Swihart & Girshick [44] also observed that the critical temperature for the onset of nucleation was substantially higher in a hydrogen atmosphere than in inert one.

Vapor phase reaction method. The most commonly used chemical process for silicon microspheres production is the vapor phase reaction method. The decomposition of a silicon-containing precursor is induced by heating at the decomposition temperature, and the SiH_4 (silane) or trichlorosilane $SiHCl_3$ gases undergo the following reactions as Eq. 1 and Eq. 2:

$$SiH_4 \rightarrow Si + 2H_2 \quad (1)$$

$$SiHCl_3 + H_2 \rightarrow Si + 3HCl \quad (2)$$

Particle synthesis is conducted in the gas-phase either in static [45] or in flow reactors [46, 47]. The static reactors process offers some advantages over the flow reactor one, such as simpler process and higher quality microspheres, however it is a non-continuous process, so that flow reactors are more widely used. The main advantages of using flow reactor are the high-throughput, continuous operation and low energy costs [48]. Wu *et al.* [41] also reported the synthesis of spherical silicon particles by rate-controlled thermal decomposition of silane in a vertical flow reactor. Fig. 3 shows the schematic diagram of their apparatus which consists of an 850 mm long quartz tube that is heated in five separate zones. The reactor was designed as to assure that the initial reaction rate could be kept at very low values, in order to severely limit the size and number concentration of particles generated by nucleation. In their procedure, the temperature of the reactor wall is gradually increased, with the first reaction zone heated to 770 K and the fifth one to 1523 K. By increasing the temperature along the length of the flow reactor, silane decomposes sufficiently slow and complete decomposition is assured to facilitate control of the structure and the crystalline state of the particles. The powders generated by this flow reactor consisted of high-purity, spherical, non-agglomerated, and uniformly sized particles. Most of the particles were crystalline. Fig. 4 shows the Transmission Electron Microscopy image of the silicon microspheres.

Onischuk *et al.* [49] also performed experiments to synthesize spherical silicon particles in vertical flow reactor, with the aim of investigating the mechanism of aerosol formation during thermal decomposition of silane. Fig. 5 shows the schematic diagram of their experimental set-up.

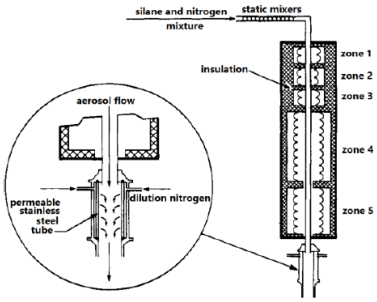

Fig. 3 Schematic diagram of the vertical flow reactor used by Wu *et al.* [41]

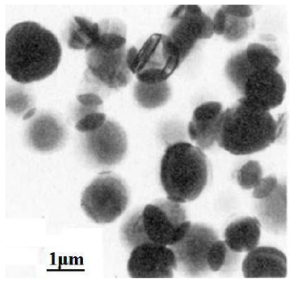

Fig. 4 TEM image of the crystalline silicon particles produced by the flow reactor [41].

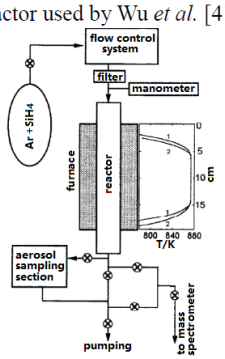

Fig. 5 Schematic diagram of the experimental set-up used by Onischuk *et al.* [49]

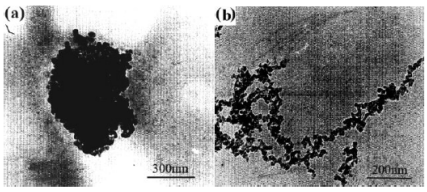

Fig. 6 TEM images of compact aggregates at T < 830K (a) and chain-like aggregates at T > 830 K (b) [49]

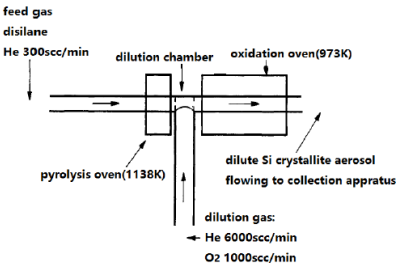

Fig. 7 Schematic diagram of the horizontal flow reactor used by Littau *et al.* [42]

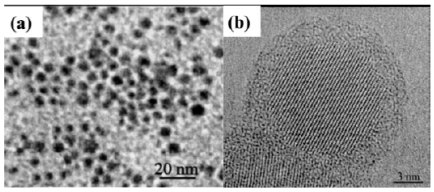

Fig. 8 TEM image (a) and HREM image (b) of single-crystalline silicon particles [50]

Before entering the reactor, a mixture of silane and argon was let through an aerosol filter and the gas flow rate was varied in the range 5.1-16.3 cm^3 s^{-1} (at 293 K and 39 kPa). The mixture was thermally decomposed at temperatures between 790K and 1000 K. As shown in Fig. 6, compact aggregates were observed at T < 830K, whereas chain-like ones were found at T > 830 K.

A horizontal flow reactor was reported by Littau *et al.* and Fig. 7 shows the schematic diagram of their apparatus [42]. The reactor has three sections where, respectively, initial pyrolysis, particle dilution, and surface oxidation take place. The precursor was diluted to 3-30 ppm in Helium gas and the pyrolysis temperature was 1138K. The microspheres generated by this technique exhibited a core-shell structure: the 13 nm core of crystalline silicon was capped with an approximately 1.5 nm shell of amorphous silicon dioxide

Huisken *et al.* [50] reported that the CO laser-induced decomposition of silane in a flow reactor also yielded spherical core-shell particles with diameters between 2 and 20 nm. Fig. 8 (a) shows a TEM micrograph of the obtained particles. Remarkably, the particles produced in the pulsed mode did not agglomerate to larger aggregates. This is ascribed to the early extraction of the nanoparticles from the reaction zone and their fast cooling in the supersonic expansion with helium carrier gas. Moreover, the size distribution of the particles was narrowed by using a mechanical chopper. As shown in Fig. 8 (b), High-Resolution Electron Transmission micrographs indicates that the silicon nanoparticles produced in this experiment also consisted of a perfect monocrystalline core surrounded by a shell of silicon oxide.

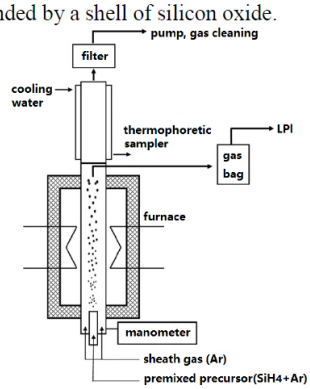

Fig. 9 Schematic diagram of experimental Set-up used by Körmer *et al.* [24]

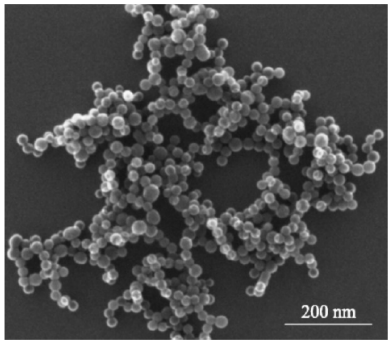

Fig. 10 SEM micrograph of monodispersed spherical silicon nanoparticles [24]

In order to prepare spherical nanoparticles with a narrow size distribution, Körmer *et al.* [24] presented experimental studies in a hot wall reactor. The design was inspired by the reactors of Kirchhof *et al.* [51] and Fernández de la Mora *et al.* [52]. Fig. 9 shows the schematic diagram of the experimental set-up used by Körmer *et al* [24]. Spherical silicon powders were obtained at a high production rate by a proper choice of the governing parameters: temperature, residence time and precursor concentration. Scanning Electron Microscopy image, as shown in Fig. 10 [24], reveals that the size of the silicon particles was in the range of 20nm~40nm with a narrow size distribution. Moreover, the X-ray diffraction pattern and HRTEM images show the particles were highly crystalline.

Vapor-solid reaction method. The synthesis of uniform particles by vapor phase reaction method, called vapor-solid reaction method, requires the use as seeds of a small number of much smaller particles [40, 53-55]. The main advantages of this approach are controlled size distribution and continuous production, whereas the drawback is the need to previously introduce seeds. A schematic illustration of this kind of fluidized bed reactor is shown in Fig. 11 [56].

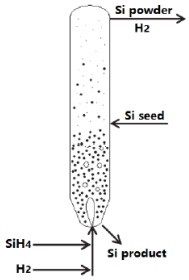

Fig. 11 Schematic diagram of fluidized bed reactor used for the vapor-solid method [56]

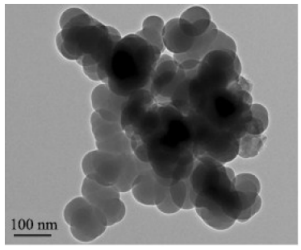

Fig. 12 TEM image of the silicon nanoparticles obtained by vapor-solid reaction method [48].

Silane and hydrogen gases enter at the bottom of the reactor with a sufficiently slow flow to fluidize the bed of silicon particles. When the silane gas is heated, it decomposes to solid silicon and gaseous hydrogen. Most of the solid silicon deposits on seeds, causing the particles to grow. While seeds are added, or generated, to ensure constant average particle size, silicon products are removed from the reactor to ensure mass balance during continuous production. Zbib *et al.* [48] reported spherical particles production by this method. Fig. 12 shows the TEM image of the obtained silicon nanoparticles. Fenollosa *et al.* [25] also demonstrated a vapor-solid reaction method to obtain silicon microspheres by high temperature decomposition of disilane gas (Si_2H_6). As shown in Fig. 13, the obtained silicon microspheres, with diameters from 0.5μm to 5μm, had perfect spherical shape and smooth surface.

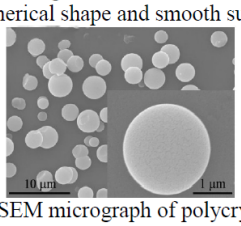

Fig. 13 SEM micrograph of polycrystalline silicon microspheres [25].

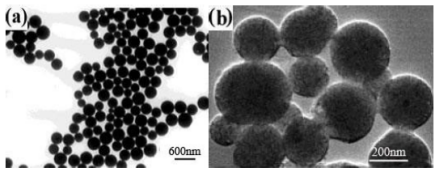

Fig. 14 TEM micrographs of the amorphous Si colloids (a) before and (b) after annealed [26].

Liquid phase reaction method. Silicon microspheres can be also obtained by a liquid phase reaction method, obtaining non-agglomerated particles with relatively narrow size distribution. However, the synthesis must be carried out in extreme reaction conditions. Pell *et al.* [26] demonstrated that trisilane pyrolysis in supercritical hexane at temperatures ranging from 673K to 773K and pressures up to 345 bar yielded amorphous silicon colloids with average diameters ranging from 50nm to 500 nm depending on the reaction conditions. Fig. 14 shows TEM (A) and SEM (B) micrographs of the amorphous Si colloids. It was found that the amorphous silicon colloids were spherical and non-agglomerated. Relatively narrow particle size distributions with standard deviations as low as ~±10% was measured by TEM. The amorphous silicon colloids were annealed after isolation from the reactor and crystallization occurred at temperatures as low as 923K. the crystalline silicon particles were also spherical and non-agglomerated. Trisilane pyrolysis in supercritical hexane provides a new approach for the synthesis of a variety of high quality silicon microspheres.

Magnesiothermal reduction method. As a promising synthesis method to obtain silicon microspheres, a metal thermal reduction process proposed by Zhu *et al.* [27] has currently received special interest. A mixture of magnesium powder and MCM-48 silica microspheres was placed in a ceramic boat and inserted into a tube furnace, which was then heated to 893K in vacuum for 2h. The products were immersed in HCl solution for 6h at room temperature and were then exposed to a HF solution for 10 min to ensure that any oxide and excessive Mg powder were completely eliminated. At last the final products were obtained after drying at 373K for 4h. SEM images of the original MCM-48 silica beads (a) and the as-synthesized mesoporous silicon microspheres (b) are shown in Fig. 15: it can be seen that the original spherical shape and size are well preserved after reduction and the subsequent treatments [27].

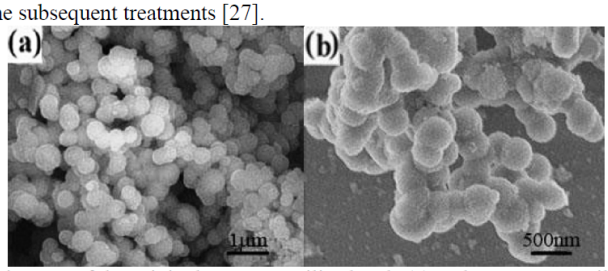

Fig. 15 SEM images of the original MCM-48 silica beads (a) and mesoporous silicon (b) [27].

Lu & Zhang [21] also obtained spherical silicon particles by a different magnesiothermal reduction process. First silica spherical particles were prepared through hydrolysis of tetraethylorthosilicate (TEOS). Then the obtained product was mixed with magnesium powder and heat-treated at 1173K for 3h under argon atmosphere to reduce silica. The final particles were obtained after the treatment with 10 *wt.* % HCl solution and alcohol, and after drying at 333K in vacuum. Since the pH value of TEOS during hydrolysis determines the silicon morphology, spherical particles could be controllably synthesized by adjusting this parameter. Fig. 16 shows a SEM image of the final silicon microspheres with a size around 400 nm [21].

Xie *et al.* [22] reported the synthesis of spherical porous silicon using the same approach as that employed by Lu & Zhang. Magnesiothermal reduction was performed at 973K-1173K for 12h in flowing Ar atmosphere. When the reaction temperature was above 1073K, the reaction products were silicon and removable MgO byproduct, while it was possible to avoid Mg_2SiO_4 formation. MgO and residual SiO_2 were easily removed by acid etching. The morphology of the SiO_2 precursor and that of the magnesiothermal reduction product is shown in Fig. 17 [22]. It was found that the original spherical morphology of the SiO_2 particles, as well as the monodisperse distribution of sizes, could be preserved during the magnesiothermal reduction.

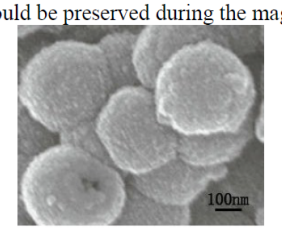

Fig. 16 SEM image of the silicon microspheres obtained by Lu & Zhang by using a magnesiothermal method [21].

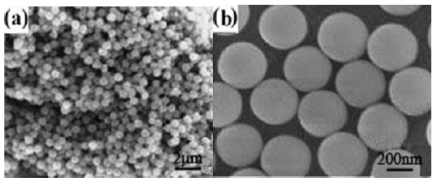

Fig. 17 SEM images of the magnesiothermal reduction product (a) and the SiO_2 precursor (b) [22].

Mechanisms of formation of silicon microspheres produced by decomposition of silicon hydride.

In order to improve the manufacture techniques of silicon microspheres, the understanding of their formation mechanism is absolutely crucial, for it allows one to control the parameters which govern particle size and morphology. Various mechanisms of particle formation by silane pyrolysis have been proposed (44, 57-62). Silicon microspheres are formed by a series of complex processes including gas-phase reaction, nucleation, particle growth, and restructuring. This process is illustrated in Fig. 18.

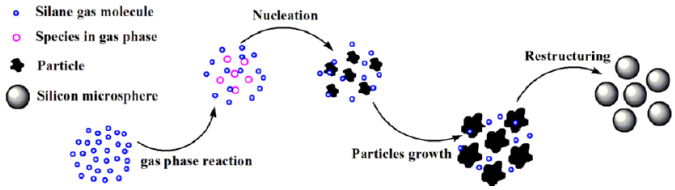

Fig. 18 Schematic diagram for silicon microspheres formation

Much work has been undertaken on the mechanism involved in the first step, i.e. the gas-phase reaction of silane. Hogness *et al.* [63] first studied this reaction and reported that silane decomposed into silicon and hydrogen by a single-step reaction. However, Purnell and Walsh proposed that the thermal decomposition of silane be a multi-body reaction and that the gaseous products in the very early stages of the reaction are hydrogen, disilane and trisilane [64]. Since then, the mechanism for the gas-phase reaction of silane has been widely studied. The present general view is that the gas-phase reaction is a complex event and that the decomposition process can proceed through a

series of intermediate gas-phase species, such as silenes, silylenes, silylanions and three-dimensional polycyclic silicon hydride species [44, 57, 58, 60], which eventually will give rise to particle formation. For example, Yuuki *et al.* [65] proposed a particle formation mechanism that included species containing up to five silicon atoms and the formation of particles from Si_5H_{12}, whereas Swihart and Girshick arrived to 2615 reactions and 221 silicon hydride species, up to Si_{20} [44]. As a matter of fact, the actual reaction will depend on a number of parameters, like silane concentration, temperature, and pressure [40].

Various models have been proposed to describe the second step of particles formation, i.e. particle nucleation during thermal decomposition of silane [66, 67]. Several researchers established models for homogeneous nucleation of pure silicon from its supersaturated vapor [68-70]. They suggested that formation of supersaturated silicon vapor in the gas-phase was the driving force for nucleation during silane pyrolysis. For example, Herrick & Woodruff [69] calculated the homogeneous nucleation rates of solid silicon and compared their results with experimental values, showing that the nucleation rate is determined by a very large super-saturation and a very small concentration of silicon vapor at lower temperatures, whereas in the high temperature range the super-saturation is small and the concentration of silicon vapor is large. Moreover Tao & Hunt [43] showed that inert ambient and low pressure promoted nucleation of Si_3 as shown in Fig. 19.

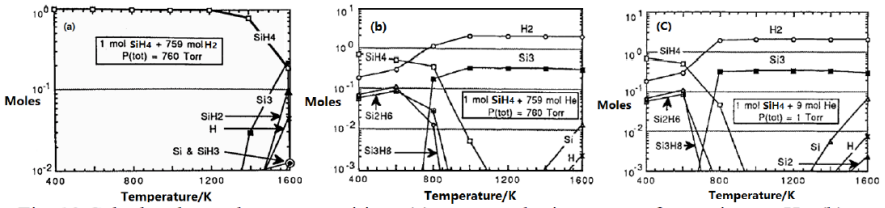

Fig. 19 Calculated gas-phase compositions (a) at atmospheric pressure for carrier gas H_2, (b) at atmospheric pressure for carrier gas He and (c) at a low pressure for carrier gas He.

However, such models did not explain the experimental observation that particles formed during silane pyrolysis contained hydrogenated silicon groups. It is generally accepted that the particles are formed by a chemical nucleation process [44, 58]. Particle inception (nucleation) is induced by a collision and activation of the chemical species from gas-phase such as a silylene species with another silylene or silene species. For example Menz *et al.* [71] showed a model including inception reactions that led to formation of particles. Other similar mechanisms for particle formation by silicon hydride clustering were also presented [44, 57, 60, 65]. A general inception reaction can be described by Eq. 3.

$$Si_iH_j + Si_kH_l \rightarrow P \ (\eta_{Si} = i + K, \ \eta_H = j + l) \tag{3}$$

Where the left-hand species Si_iH_j and Si_kH_l are in the gas-phase, the right-hand species P is a newly formed particles with Si number of silicon atoms and H that of hydrogen atoms. Körmer *et al.* [61] suggested that the stable nuclei must have a size larger than the critical nucleus diameter, representing the threshold above which gas-phase molecular clusters could convert to particles. When the diameter of the gas-phase clusters exceeds the critical nucleus diameter, particle nuclei are formed. On the basis of the above mechanism Menz *et al.* [71] concluded that the smallest particle nucleus is a Si_2 molecule and that the corresponding gas-phase species is silene (Si_2H_4A). However, Swihart *et al.* suggested that molecular clusters with more than 10 silicon atoms can be considered to be particles [44]. The rate of inception was calculated using the transition kernel:

$$R_{inception} = 0.5K^{tr}N^2C(S_iH_j)C(Si_kH_l) \tag{4}$$

Where K_{tr} is the transition regime coagulation kernel, C (Si_iH_j) and C (Si_kH_l) is the gas-phase concentrations of the colliding species, and N is Avogadro's number.

Once particles are formed in the gas phase, subsequent particle growth may occur through surface reaction or condensation [58, 62, 71]; this represents the third step of the silicon

microspheres formation process described in Fig.18. As described in Eq. 5, growth by surface reaction refers to the heterogeneous reaction of gas-phase species on the surface of existing particles with hydrogen release:

$$P_i(\eta_{Si}, \eta_H) + Si_iH_{2i+2} \rightarrow P(\eta_{Si}+i, \eta_H+2) + iH_2 \quad (5)$$

Menz *et al.* proposed [62] that the rate of a surface reaction process might be modelled as an Arrhenius process and that it is also proportional to the surface area of the particle, S_q:

$$R_{SR} = AS_qC(Si_iH_{2i+2})\exp(-E_A/RT) \quad (6)$$

Where R_{SR} is the rate of a surface reaction process, E_A and A are the Arrhenius parameters for silicon hydrides Si_iH_{2i+2} in the gas-phases, and C (Si_iH_{2i+2}) is the concentration of silicon hydrides Si_iH_{2i+2}. Particles could also undergo a growth process due to condensation reaction of silicon hydrides from the super saturated vapor, as described in Eq. 7:

$$P_i(\eta_{Si}, \eta_H) + Si_iH_j \rightarrow P(\eta_{Si}+i, \eta_H+j) \quad (7)$$

The condensation process of silicon hydrides on the particle surface was described by Sander *et al.* [72] as a collisional process, so that the rate of reaction is given by a collision kernel. Following these calculation, condensation led to an increase of particle volume and increased the sphericity. Körmer *et al.* [61] confirmed that the occurrence of condensation plays an important role on formation of silicon nanoparticles with narrow size distributions. Celnik *et al.* [73] proposed that the growth rate due to the condensation process can be calculated according to:

$$R_{cond} = 2.2\eta C\sqrt{\frac{\pi k_B T}{2m}}(d + d_c)^2 \quad (8)$$

Where η denotes the efficiency of the collision; C, m, and d denote the gas-phase concentration, mass, and collision diameter of the condensing species, respectively; k_B is Boltzmann's constant; and d_c denotes the collision diameter of the particle.

According to Kirchhof *et al.* [51], as the particle size increases, particles restructure to form spherical silicon by particle coagulation accompanied by sintering (last step in Fig. 18). The coagulation and the sintering processes determine the shape and the size of the final particles [51]. Sintering reduces the particle surface, minimizing the free energy, and making them rounder, whereas coagulation decreases their sphericity [72]. Wu *et al.* [41] obtained highly-spherical crystalline silicon particles through coagulation and sintering of smaller particles at a high temperature, the latter causing coalescence, and yielding spherical particle. Coagulation was also considered as the result of collision and subsequent adhesion of two primary particles. Sander *et al.* [72] proposed that the coagulation rate R_{coag} of two particles P_i and P_j is proportional to the free molecular collision kernel:

$$K^{fm}(i, j) \propto \left(\frac{1}{m_i} + \frac{1}{m_j}\right)^{0.5}(d_{c,i} + d_{c,j})^2 \quad (9)$$

Where m represents the mass and d_c represents the collision diameter.

However, Onischuk *et al.* [60] proposed that the coagulation constant K (i, j) for the two particles is set as:

$$K(i, j) = \left(\frac{1}{K^{\alpha}(i, j)} + \frac{1}{K^{D}(i, j)}\right)^{-1} \quad (10)$$

Where K^{α} (i, j) is the rate constant of the free-molecular coagulation and K^{D} (i, j) is the rate constant for the diffusion-controlled coagulation. The rate constant for diffusion controlled coagulation is represented as:

$$K^{D}(i, j) = 4\pi(r_i + r_j)(d_i + d_j) \quad (11)$$

Where r_i and r_j are the radii of the colliding particles, d_i and d_j are the diffusion coefficients of these particles. Menz *et al.* [62] proposed that the rate constant of coagulation be given by the transition kernel, with the transition regime coagulation kernel K_{tr} represented as:

$$K^{tr}(i, j) = \left(\frac{1}{K^{fm}(i, j)} + \frac{1}{K^{sf}(i, j)}\right)^{-1} \quad (12)$$

Where $K^{fm}(i, j)$ is the free molecular collision kernel and $K^{sf}(i, j)$ is the slip flow kernel. The equation is similar to that proposed by Onischuk *et al.* [60].

The term sintering refers to the coalescence of connected particles through neck formation by solid-state diffusion. The sintering rate R_{sinter} depends mainly on the excess surface of the particles in respect to their equivalent spherical particle. The asymptotic equation describing the sintering of a particle was presented by Koch & Friedlander [74]. It is expressed in the form:

$$\frac{da}{dt} \propto -\frac{1}{\tau}(a - a_{final}) \quad (13)$$

Where a denotes the surface of the two primary particles; a_{final} denotes their equivalent spherical surface area; and τ denotes a characteristic sintering time which is related to the time required for two neighboring primary particles to coalesce.

When the particle restructures to form spherical ones, hydrogen evolution occurs; for example, Onischuk *et al.* [60] proposed hydrogen evolution from SiH and SiH_2 groups belonging to the particles to form silicon particles. Menz *et al.* [62] suggested that release of hydrogen from particles be a stochastic jump process and could be considered as a hydrogen desorption process. Sinniah *et al.* [75] showed that the rate of hydrogen desorption is proportional to the coverage of hydrogen (first-order reaction). Based on their study, Menz *et al.* [62] proposed that the rate of hydrogen desorption could be given described by:

$$R_{H_2} = A_{H_2}\theta_q \exp(-E_{A,\ H_2}/RT) \quad (14)$$

Where A_{H_2} and $E_{A,\ H_2}$ are the Arrhenius parameters, and θ_q is the hydrogen coverage.

Outlook

Various methods have been developed for the synthesis of silicon microspheres and substantial research has been done in order to improve the quality and the yield of their production. However, there are still many challenges to be tackled by current approaches. Furthermore, the formation of silicon nanoparticles is becoming more and more important in the production of powder catalysts, ceramics, nano-electronic devices, etc. Therefore a major issue is presently to devise methods to obtain nano-sized silicon particles. The particles should be uniformly sized to generate high quality. Another challenge is that the product yields of spherical silicon particles are usually low, limiting their practical application.

Acknowledgments

This work has been financed by National Science Foundation of China (Grant No. 51474014).

References

[1] S. M. Sze, Physics of semiconductor devices, second ed., Wiley, New York, 1981.

[2] B. G. Streetman, S. Banerjee, Solid State Electronic Devices, fifth ed., Prentice Hall, New Jersey, 2000.

[3] Ali. Serpengüzel, A. Kurt and U. K. Ayaz, Silicon microspheres for electronic and photonic integration, Photonics and Nanostructures-Fundamentals and Applications 6(2008)179-182.

[4] O. Painter, R. K. Lee, A. Scherer, A. Yariv, J. D. O'Brien, P. D. Dapkus, Two-dimensional photonic band-gap defect mode laser, Science. 284(1999)1819-1821.

[5] A. Blanco, E. Chomski, S. Grabtchak, M. Ibisate, S. John, S.W. Leonard, Large scale synthesis of a silicon photonic crystal with a complete three dimensional bandgap near 1.5 micrometers, Nature. 405(2000)437-440.

[6] B. S. Song, S. Noda and T. Asano, Photonic devices based on in-plane hetero photonic crystals, Science. 300 (2003)1537-1537.

[7] A. Liu, H. Rong, M. Paniccia, O. Cohen, D. Hak, Net optical gain in a low loss silicon-on-insulator waveguide by stimulated Raman scattering, Optics Express. 12(2004) 4261-4268.

[8] H. Rong, A. Liu, R. Nicolaescu, M. Paniccia, Raman gain and nonlinear optical absorption measurements in a low-loss silicon waveguide, Applied Physics Letters. 85 (2004)2196-2198.

[9] R. Jones, H. Rong, A. Liu, A. Fang, M. Paniccia, Net continuous wave optical gain in a low loss silicon-on-insulator waveguide by stimulated Raman scattering, Optics Express. 13 (2005) 19-25.

[10] J. Song, Y. Li, X. Zhou, X. Li, Planar grating multiplexers using silicon nanowire technology: numerical simulations and fabrications, Progress in Electromagnetics Research. 123 (2012) 509-526.

[11] H. Rong, R. Jones, A. Liu, O. Cohen, D. Hak, A. Fang, A continuous-wave Raman silicon laser, Nature. 433 (2005) 725-728.

[12] K. J. Vahala, Optical microcavities, Nature. 424 (2003) 839-846.

[13] T. Minemoto, C. Okamoto, S. Omae, M. Murozono, H. Takakura, Y. Hamakawa, Fabrication of spherical silicon solar cells with semi-light-concentration system, Japanese Journal of Applied Physics. 44(2005)4820-4824.

[14] T. Minemoto, H. Takakura, Fabrication of spherical silicon crystals by dropping method and their application to solar cells, Japanese Journal of Applied Physics. 46(2007) 4016-4020.

[15] T. Ikuta, T. Minemoto, H. Takakura, Y. Hamakawa, Optical design of spherical silicon solar cells with reflector cup, Japanese Journal of Applied Physics. 45 (2006) 3938-3942.

[16] S. Omae, T. Minemoto, M. Murozono, H. Takakura, Y. Hamakawa, Crystal characterization of spherical silicon solar cell by X-ray diffraction, Japanese Journal of Applied Physics. 45 (2006) 3933-3937.

[17] H. C. Tapalian, J. P. Laine, P. A. Lane, Thermooptical switches using coated microsphere resonators, IEEE Photonics Technology Letters. 14 (2002) 1118-1120.

[18] I. Teraoka, S. Arnold, and F. Vollmer, Perturbation approach to resonance shifts of whispering-gallery modes in a dielectric microsphere as a probe of a surrounding medium, Journal of the Optical Society of America B. 20 (2003)1937-1946.

[19] A. B. Matsko, A. A. Savchenkov, V. S. Ilchenko, L. Maleki, Optical gyroscope with whispering gallery mode optical cavities, Optics Communications. 233 (2004) 107-112.

[20] Y. O. Yilmaz, A. Demir, A. Kurt, A. Serpenguzel, Optical channel dropping with a silicon microsphere, IEEE Photonics Technology Letters. 17 (2005) 1662-1664.

[21] M. Lu, H. Zhang, Controllable synthesis of spherical silicon and its performance as an anode for lithium-ion batteries, Ionics. 19 (2013) 1695-1698.

[22] J. Xie, G. Wang, Y. Huo, S. Zhang, G. Cao, X. Zhao, Nanostructured silicon spheres prepared by a controllable magnesiothermic reduction as anode for lithium ion batteries, Electrochimica Acta. 135 (2014) 94-100.

[23] S. Omae, T. Minemoto, M. Murozono, H. Takakura, Y. Hamakawa, Crystal growth mechanism of spherical silicon fabricated by dropping method, Japanese Journal of Applied Physics. 45(2006)3577-3580.

[24] R. Körmer, M. Jank, H. Ryssel, H. J. Schmid, W. Peukert, Aerosol synthesis of silicon nanoparticles with narrow size distribution-part 1: Experimental investigations, Journal of Aerosol Science. 41 (2010) 998-1007.

[25] R. Fenollosa, F. Meseguer, M. Tymczenko, Silicon colloids: from micro-cavities to photonic sponges, Advanced Materials. 20 (2008) 95-98.

[26] L. E. Pell, A. D. Schricker, F. V. Mikulec, B. A. Korgel, Synthesis of amorphous silicon colloids by trisilane thermolysis in high temperature supercritical solvents, Langmuir. 20 (2004) 6546-6548.

[27] J. Zhu, R. Liu, J. Xu, C. Meng, Preparation and characterization of mesoporous silicon spheres directly from MCM-48 and their response to ammonia, Journal of Materials Science. 46(2011) 7223-7227.

[28] S. Omae, C. Okamoto, H. Takakura, Y. Hamakawa, M. Murozono, Crystal structure analysis of spherical silicon using X-Ray pole figures, Solid State Phenom. 93 (2003) 249-256.

[29] X. Huang, S. Uda, H. Tanabe, N. Kitahara, H. Arimune, K. Hoshikawa, In situ observations of crystal growth of spherical Si single crystals, Journal of Crystal Growth. 307 (2007) 341-347.

[30] S. Omae, T. Minemoto, M. Murozono, H. Takakura, Y. Hamakawa, Crystal evaluation of spherical silicon produced by dropping method and their solar cell performance, Solar Energy Materials & Solar Cells. 90 (2006) 3614-3623.

[31] Z. Liu, T. Nagai, A. Masuda, M. Kondo, K. Sakai, K. Asai, Seeding method with silicon powder for the formation of silicon spheres in the drop method, Journal of Applied Physics. 101 (2007) 093505(1-5).

[32] C. Okamoto, T. Minemoto, M. Murozono, H. Takakura, Y. Hamakawa, Electric and crystallographic characterizations on hydrogen passivated spherical silicon solar cells, Japanese Journal of Applied Physics. Part 1, 44 (2005) 7372-7376.

[33] C. Okamoto, K. Tsujiya, T. Minemoto, M. Murozono, H. Takakura, Y. Hamakawa, Reduction in dislocation density of spherical silicon solar cells fabricated by decompression dropping method, Japanese Journal of Applied Physics. Part 1, 44 (2005) 8351-8355.

[34] Z. Liu, K. Asai, A. Masuda, T. Nagai, Y. Akashi, M. Murozono, Improvement of the production yield of spherical Si by optimization of the seeding technique in the dropping method, Japanese Journal of Applied Physics. 46(2007) 5695-5700.

[35] Y. Kuzuokaa, S. Isomaeb, and Y. Yamaguchi, Crystal morphology of spherical silicon particles produced by jet-splitting method, Journal of Crystal Growth. 304 (2007) 487-491.

[36] M. Gharghi, S. Sivoththaman, Growth and structural characterization of spherical silicon crystals grown from polysilicon, Journal of Electronic Materials. 37 (2008) 1657-1664.

[37] S. Ueno, H. Kobatake, H. Fukuyama, S. Awaji, H. Nakajima, Formation of silicon hollow spheres via electromagnetic levitation method under static magnetic field in hydrogen–argon mixed gas, Materials Letters. 63(2009) 602-604.

[38] S. P. Walch, C. E. Dateo, Thermal decomposition pathways and rates for silane, chlorosilane, dichlorosilane and trichlorosilane, Journal of Physical Chemistry. 105 (2001) 2015-2022.

[39] W. A. P. Claasen, J. Bloem, The nucleation of CVD silicon on SiO_2 and Si_3N_4 substrates, Journal of the Electrochemical Society. 127 (1980) 194-202.

[40] W. O. Filtvedt, A. Holt, P. A. Ramachandran, M. C. Melaaen, Chemical vapor deposition of silicon from silane: Review of growth mechanisms and modeling / scale up of fluidized bed reactors, Solar Energy Materials & Solar Cells. 107(2012) 188-200.

[41] J. J. Wu, H. V. Nguyen, R. C. Flagan, A method for the synthesis of submicron particles, Langmuir. 3(1987) 266-271.

[42] K. A. Littau, P. J. Szajowski, A. J. Muller, A. R. Kortan, L. E. Bm, A luminescent silicon nanocrystal colloid via a high-temperature aerosol reaction, The Journal of Physical Chemistry. 97 (1993) 1224-1230.

[43] M. Tao, L. P. Hunt, The thermodynamic behavior of the Si-H system and its role in Si CVD from SiH_4, Journal of the Electrochemical Society. 139(1992) 806-809.

[44] M. T. Swihart, S. L. Girshick, Thermochemistry and kinetics of silicon hydride cluster formation during thermal decomposition of silane, The Journal of Physical Chemistry B. 103(1999) 64-76.

[45] N. K. Serdyuk, V. P. Strunin, E. N. Chesnokov, V. N. Panfilov, Isotope exchange during thermal decomposition of the mixture SiH_4 + SiD, Kinetikai Kataliz (Russia). 26(1985) 790-798.

[46] R. Becerra, R. Walsh, Some mechanistic problems in the kinetic modeling of monosilane pyrolysis, The Journal of Physical Chemistry. 96 (1992) 10856-10862.

[47] A. A. Onischuk, V. P. Strunin, M. A. Ushakova, V. N. Panfilov, Aerosol particles under silane pyrolysis, Chemical Physics (Russia). 13(1994)129-138.

[48] M. B. Zbib, U. Sahaym, and D. Bahri, Characterization of silicon nanoparticles formed from a fluidized bed reactor and their incorporation onto metal-coated carbon fibers, Journal of metals. 66(2014) 82-86.

[49] A. A. Onischuk, V. P. Strunin, M. A. Ushakova, V. N. Panfilov, On the pathways of aerosol formation by thermal decomposition of silane, Journal of Aerosol Science. 28(1997) 207-222.

[50] F. Huisken, H. Hofmeister, B. Kohn, M. A. Laguna, V. Paillard, Laser production and deposition of light-emitting silicon nanoparticles, Applied Surface Science. 154-155(2000)305-313.

[51] M. J. Kirchhof, H. J. Schmid, W. Peukert, Reactor system for the study of high-temperature short-time sintering of nanoparticles, Review of Scientific Instruments. 75(2004) 4833-4840.

[52] J. Fernández de la Mora, N. Rao, P. H. Mc Murry, Inertial impaction of fine particles at moderate Reynolds numbers and in the transonic regime with a thin-plate orifice nozzle, Journal of Aerosol Science. 21 (1990) 889-909.

[53] S. Balaji, J. Du, C. M. White, B. E. Ydstie, Multi-scale modeling and control of fluidized beds for the production of solar grade silicon, Powder Technology. 199(2010) 23-31.

[54] J. Du, B. E. Ydstie, Modeling and control of particulate processes and application to poly-silicon production, Chemical Engineering Science. 67(2012) 120-130.

[55] S. K. Iya, U.S. Patent, 4,684,513. (1987).

[56] C. M. White, P. Ege and B. E. Ydstie, Size distribution modeling for fluidized bed solar-grade silicon production, Powder Technology. 163(2006) 51-58.

[57] M. Frenklach, L. Ting, H. Wang, M. J. Rabinowtiz, Silicon particle formation in pyrolysis of silane and disilane, Israel Journal of Chemistry. 36 (1996) 293-303.

[58] P. Ho, M. E. Coltrin, W. G. Breiland, Laser-induced fluorescence measurements and kinetic analysis of Si atom formation in a rotating disk chemical vapor deposition reactor. Journal of Physical Chemistry, 98(1994) 10138-10147.

[59] C. Hollenstein, J. L. Dorier, J. Dutta, A. A. Howling, Diagnostics of particle genesis and growth in RF silane plasmas by ion mass spectrometry and light scattering, Plasma Sources Science & Technology. 3(1994) 278-285.

[60] A. A. Onischuk, A. I. Levykin, V. P. Strunin, K. K. Sabelfeld, V. N. Panfilov, Aggregate formation under homogeneous silane thermal decomposition, Journal of Aerosol Science. 31(2000), 1263-1281.

[61] R. Körmer, H. J. Schmid, and W. Peukert, Aerosol synthesis of silicon nanoparticles with narrow size distribution-Part 2: Theoretical analysis of the formation mechanism, Journal of Aerosol Science. 41 (2010) 1008-1019.

[62] W. J. Menz, M. Kraft, A new model for silicon nanoparticle synthesis, Combustion and Flame. 160(2013) 947-958.

[63] T. Hogness, T. Wilson, and W. Johnson, The thermal decomposition of silane, Journal of the American Chemical Society. 58(1936) 108-112.

[64] J. H. Purnell, R. Walsh, The pyrolysis of monosilane, Proceedings of the Royal Society Series A. 293(1966) 543-561.

[65] A. Yuuki, Y. Matsui and K. Tachibana, A numerical study on gaseous reactions in silane pyrolysis, Japanese Journal of Applied Physics. 27 (1987) 747-754.

[66] H. V. Nguyen, R. C. Flagan, Particle formation and growth in single-stage aerosol reactors, Langmuir. 7(1991) 1807-1814.

[67] F. Slootman, J. Parent, Homogeneous gas-phase nucleation in silane pyrolysis, Journal of Aerosol Science. 25 (1994) 15-21.

[68] S. L. Girshick, C. P. Chiu, Homogeneous nucleation of particles from the vapor phase in thermal plasma synthesis, Plasma Chemistry & Plasma Processing. 9(1989) 355-369.

[69] C. S. Herrick, D. W. Woodruff, The homogeneous nucleation of condensed silicon in the gaseous Si-H-Cl system, Journal of the Electrochemical Society. 131 (1984) 2417-2422.

[70] F. E. Kruis, J. Schoonman and B. Scarlett, Homogeneous nucleation of silicon, Journal of Aerosolence. 25(1994) 1291-1304.

[71] W. J. Menz, S. Shekar, G. Brownbridge, S. Mosbach, R. Körmer, W. Peukert, Synthesis of silicon nanoparticles with a narrow size distribution: A theoretical study, Journal of Aerosol Science. 44 (2012) 46-61.

[72] M. Sander, R. H. West and M. S. C. M. Kraft, A detailed model for the sintering of poly-dispersed nanoparticle agglomerates, Aerosol Science & Technology. 43(2009), 978-989.

[73] M. Celnik, R. Patterson, M. Kraft, W. Wagner, Coupling a stochastic soot population balance to gas-phase chemistry using operator splitting, Combustion and Flame. 148(2007) 158-176.

[74] W. Koch, S. K. Friedlander, The effect of particle coalescence on the surface area of a coagulating aerosol, Journal of Aerosol Science. 140(1990), 419-427.

[75] K. Sinniah, M. G. Sherman, L. B. Lewis, W. H. Weinberg, J. T. J. Yates, K. C. Janda, Hydrogen desorption from the monohydride phase on Si(100), Journal of Chemical Physics. 92 (1990) 5700-5711.